Field ion microscopic studies of the CO oxidation on platinum: Field ion imaging and titration reactions

Cite as: J. Chem. Phys. **100**, 6907 (1994); https://doi.org/10.1063/1.467006
Submitted: 06 August 1993 • Accepted: 06 January 1994 • Published Online: 31 August 1998

V. Gorodetskii, W. Drachsel and J. H. Block

Field ion microscopic studies of the CO oxidation on platinum: Field ion imaging and titration reactions

V. Gorodetskii,[a] W. Drachsel, and J. H. Block
Fritz-Haber-Institut der Max-Planck-Gesellschaft Faradayweg 4-6, Dahlem, D-14195 Berlin, Germany

(Received 6 August 1993; accepted 6 January 1994)

Elementary steps of the CO oxidation—which are important for understanding the oscillatory behavior of this catalytic reaction—are investigated simultaneously on different Pt-single crystal surfaces by field ion microscopy. Due to preferential ionization probabilities of oxygen as imaging gas on those surface sites, which are adsorbed with oxygen, these sites can be imaged in a lateral resolution on the atomic scale. In the titration reaction a CO_{ad}-precovered field emitter surface reacts with gaseous oxygen adsorbed from the gas phase or, vice versa, the O_{ad}-precovered surface with carbon monoxide adsorbed from the gas phase. The competition of the manifold of single crystal planes exposed to the titration reaction at the field emitter tip is studied. The surface specificity can be documented in the specific reaction delay times of the different planes and in the propagation rates of the reaction-diffusion wave fronts measured on these individual planes during the titration reaction with a time resolution of 40 ms. At 300 K the CO_{ad}-precovered surfaces display the {011} regions, precisely the {331} planes as the most active, followed by {012}, {122}, {001}, and finally by {111}. Reaction wave fronts move with a velocity of 8 Å/s at {012}, with ≈0.8 Å/s at {111}, and have a very fast "switch-on" reaction at the (001) plane with 500 Å/s. At higher temperature, $T=350$ K, an acceleration of reaction rates is combined with shorter delay times. The titration reaction of a precovered O_{ad} surface with CO_{gas} at $T=373$ K shows the formation of CO islands starting in the {011} regions with a quickly moving reaction front into the other surface areas without showing particular delay times for different surface symmetries. The two reverse titration reactions have a largely different character. The titration of CO_{ad} with oxygen adsorbed from the gas phase consists of three different steps, (i) the induction times, (ii) the highly surface specific reaction, and (iii) different rates of wave front propagation. The reaction of CO_{gas} with a precovered O_{ad} layer on the other hand starts with nucleating islands around the {011} planes from where the whole emitter surface is populated with CO_{ad} without pronounced surface specifity.

I. INTRODUCTION

The self-organization process in forming adsorption systems and the initiation of self-sustained long-lasting isothermal oscillations of catalytic surface reactions is one of the recent fascinating observations in surface dynamics. Several experimental and theoretical investigations have tried to elucidate the reasons for this phenomenon.[1-3] Of particular interest is the question of the elementary reaction steps which are involved in causing oscillations in the region of bi- or multistability of a dynamic system. There are many possible steps involved in these oscillation processes, such as adsorption, desorption, surface reaction, diffusion, surface phase transition, reconstruction, formation of subsurface species as well as lateral molecular interactions which result in the formation of islands, dissipative adsorption structures, target patterns, etc. It is a challenge to investigate these phenomena on a microscopic scale with field electron microscopy (FEM)[4,5] and field ion microscopy (FIM)[6] in particular since present models[7] claim a dimensionality of this phenomenon which exceeds the dimensions of surface planes of a field emitter tip. In the present work the competition of different single crystal planes in the titration reactions is studied by FIM. These stoichiometric reactions of a Langmuir–Hinshelwood mechanism—with turnover frequency 1—consist in the overall reactions

$$CO_{ad}+O_{2\,gas}\rightarrow CO_{2\,gas}+O_{ad}, \tag{1}$$

where a precovered CO_{ad} site is transferred into an O_{ad} site and, vice versa,

$$O_{ad}+2CO_{gas}\rightarrow CO_{2\,gas}+CO_{ad}. \tag{2}$$

With FIM the time dependence of O_{ad} formation or O_{ad} removal can be imaged *in situ*, preferential reaction sites can be located and reaction/diffusion fronts be imaged as explained in a recent publication.[6] From these titration reactions further conclusions will be drawn, later on, for the behavior of these surfaces under oscillatory conditions where higher turnover frequencies are involved.

II. EXPERIMENTS

A. The apparatus

Experiments were performed in an UHV chamber [Fig. 1(a)], equipped with a channel plate and a platinum field emitter which was supported by a tungsten loop welded to a movable cold finger of glass.[4] The tip temperature could be controlled within 1 K (at $78<T<500$ K). The background pressure was in the 10^{-10} mbar region. Reaction and imaging gases (CO, O_2, Ne, He) of highest purity were supplied with controlled flow rates. A quadrupole mass spectrometer con-

[a]Boreskov Institute of Catalysis of the Siberian Branch of the Russian Academy of Sciences, Novosibirsk, Russia.

 0021-9606/94/100(9)/6907/8/$6.00

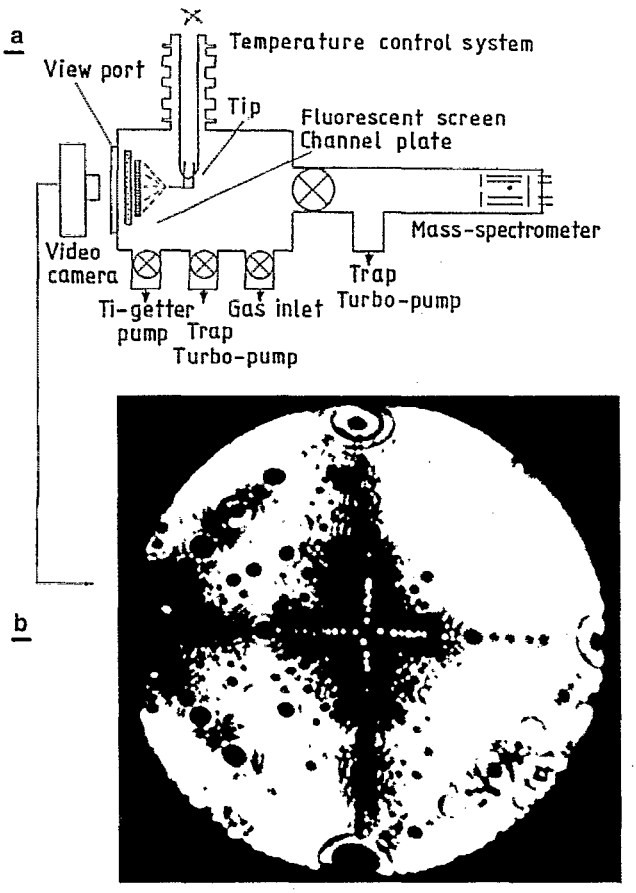

FIG. 1. (a) The UHV chamber for imaging titration reactions (or oscillations) of the CO oxidation. Field electrons in the FEM or field ions in the FIM from the tip are impinging at the detector consisting of a high sensitivity channel plate and a screen. The images are recorded by a video camera. (b) One of the Pt surfaces used in the experiments, imaged with Ne at 78 K, field evaporated at 16.5 kV, F_{Biv}=15 kV, 2×10^{-4} mbar, F=4.2 V/Å, r=680 Å.

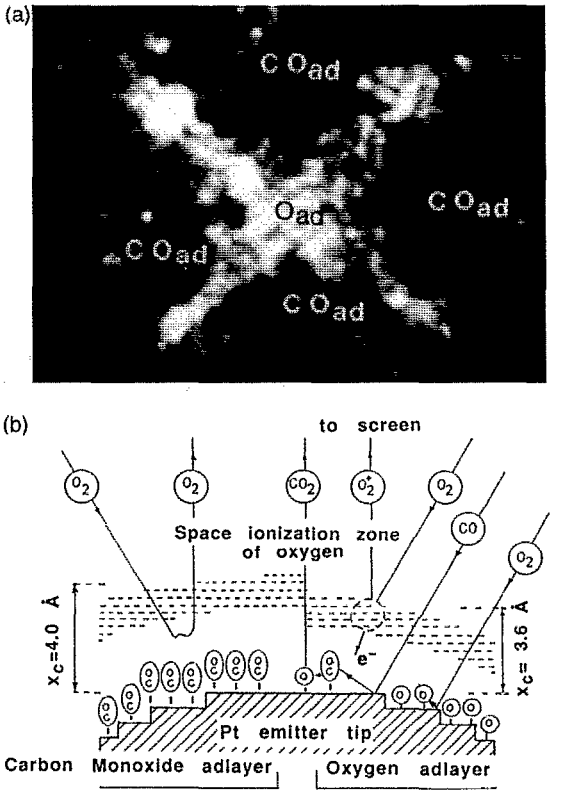

FIG. 2. (a) A field ion image of the Pt surface partially covered with O_{ad}[(001) plane and [001] vicinals] and with CO_{ad}({111} planes and surroundings). FIM image taken at T=365 K, $p_{CO}=5\times10^{-6}$ mbar, $p_{O_2}=5\times10^{-4}$ mbar, F=1.5 V/Å. The lateral resolutions enables to locate individual O_{ad} sites. (b) The field ionization process at the Pt-field emitter tip partially covered with CO_{ad} and partially with O_{ad}: Oxygen molecules are field ionized only at surface sites which are covered with O_{ad}. Ionization distances x_c differ: for $CO_{ad}\cong$4.0 Å, for $O_{ad}\cong$3.6 Å.

nected to the UHV chamber served for purity control of reaction gases. The catalyst for the CO oxidation is represented by the field evaporation end form surface of a Pt-field emitter [Fig. 1(b)] which is (001) oriented. Clean Pt surfaces were prepared by field evaporation. The FIM was operated with low ion currents (≈0.1 nA). Only at low temperatures (≈78 K) an undisturbed field ion image resolving a manifold of well-characterized high index surface planes can be expected, as in Fig. 1(b). At reaction temperatures, later on, in temperature regions of 300 to 500 K which are above the Debye temperature, lattice vibrations and surface mobilities will disturb the imaging process. It should be expected that the surfaces are then displayed in rather blurred field ion images.

During the following experiments the field ion images are continuously monitored by a CCD video camera, thus dynamic processes are investigated with a time resolution of ≈40 ms.

With this apparatus platinum surfaces are imaged *in situ* during the catalytic CO oxidation. The field emitter then is considered as an individual catalyst microcrystal which exposes various well defined single crystal surface planes simultaneously to the catalytically reacting gas. A comparison of the properties of the different single crystal planes will be possible. It is also interesting to note that groups of crystal planes with identical symmetry are located at separated remote positions of the emitter. The comparison of these crystallographically identical planes will directly give information about gas phase—or reaction diffusion front coupling of dynamic processes.

B. The imaging process

The gas mixture of CO and O_2 which reacts at the surface catalytically toward CO_2 serves at the same time as imaging gas in the field ionization process of the field ion microscope (Fig. 2). The CO oxidation proceeds via a Langmuir–Hinshelwood reaction

$$CO_{gas}+*\rightarrow CO_{ad}, \tag{3}$$

$$O_2+2*\rightarrow 2O_{ad}, \tag{4}$$

$$CO_{ad}+O_{ad}\rightarrow CO_{2\,gas}+2*, \tag{5}$$

where oxygen needs two adjacent empty sites for the dissociative adsorption. It is well known that under certain pres-

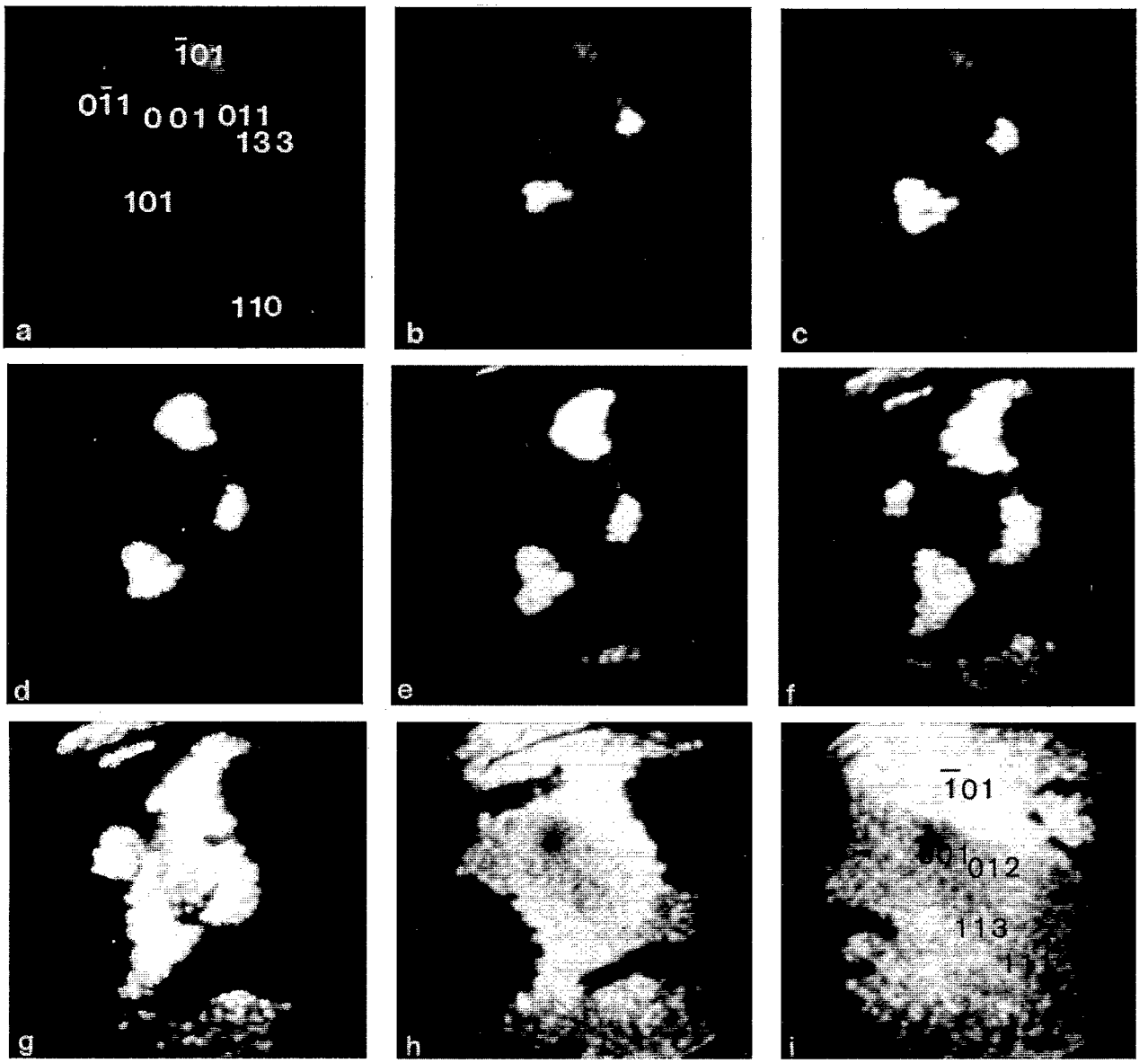

FIG. 3. FIM of the titration reaction, 300 K, at reaction times $\tau>0$ $p_{O_2} = 5 \times 10^{-4}$ mbar. Imaging voltage V_{im}=6.8 kV, $r\approx$850 Å, $F_{im}\cong$1.5 V/Å. (a) Surface precovered with CO_{ad} at $p_{CO}=5\times10^{-5}$ mbar, CO_{gas} pressure was removed at $\tau=0$; $p_{O_2} = 5 \times 10^{-4}$ mbar introduced. (b) τ=14 s after start of titration, O_{ad}=bright regions, residual $p_{CO}=1\times10^{-7}$ mbar. (c) τ=22 s; (d) τ=28 s; (e) τ=41 s; (f) τ=90 s; (g) 110 s; (h) τ=275 s; (i) τ=550 s.

sure and temperature conditions adsorption islands are formed for CO_{ad} as well as for O_{ad}. For the stability of these islands a minimum size was postulated.[7]

The ionization potentials I of the involved reaction and product gases have different values: I_{O_2} (12.06 eV)$<I_{CO_2}$ (13.76 eV)$<I_{CO}$ (14.01 eV). Thus, with increasing field strength in the beginning of a field ionization process the oxygen molecular ions will be formed first. The field ionization probability of oxygen is furthermore influenced by the adsorption layers. There may be an unknown "resonance state" for preferential O_2^+-ion formation or an influence of local work functions. The work function ϕ of platinum surfaces as determined by Fowler–Nordheim measurements in the FEM is increased when CO is adsorbed ($\Delta\phi\approx$0.7 eV) and more increased after adsorption of oxygen ($\Delta\phi\approx$1.1 eV). During the field ionization process electrons of the imaging gas enter the surface at energy levels near the Fermi level. With increasing work function the energy level for electrons, entering the solid, decreases and the barrier for electron tunneling diminishes. Thus, $O_{2\,gas}$—as the imaging gas—is preferentially imaging oxygen adsorption sites. Figure 2(b) describes these molecular interactions at the Pt surface. One part of the surface is covered with oxygen atoms O_{ad}. The minimum ionization distance X_c for the imaging gas particle, as given by

$$X_c\approx(I_p-\Phi)/F$$

(F=field strength in V/Å) is smaller for the O_{ad} sites ($X_c\approx$3.6 Å) than for the CO_{ad}-sites ($X_c\approx$4.0 Å). The applied external field strength of $F\approx$1.5 V/Å is just sufficient for field ionization of molecular oxygen at O_{ad} sites and not at

CO_{ad} sites or for CO ionization at any site. The gas phase oxygen molecules have three reaction path ways during the surface interaction.

(1) At O_{ad} sites, oxygen molecules experience a high ionization probability toward O_2^+.

(2) At empty pair sites, oxygen dissociates, chemisorbs, and eventually reacts toward $CO_{2\,gas}$.

(3) At CO_{ad} sites, O_2 molecules are reflected without being ionized at the low field of $F \approx 1.5$ V/Å.

Figure 2(a) displays a field ion image taken with oxygen imaging gas at 300 K of a Pt surface partially covered with O_{ad}, partially with CO_{ad}. The orientation of the Pt crystal corresponds to that in Fig. 1(b). The central (001) plane is covered with oxygen as well as the four [100] vicinals in direction to the {110} planes. The {111} planes and surroundings thereof are in contrast covered with CO_{ad} and are consequently not imaged by O_2^+-ion currents. The image structures in Fig. 2(a) appear less blurred than expected from surface vibrations and mobilities during the exposure at $T=300$ K. The lateral resolution of these field ion images reaches values between 3 and 6 Å. There is no doubt that individual surface sites of O_{ad} are displayed at the screen.

Local field ion currents were evaluated by measuring the local brightness of the video screen. A Si-photo diode with an active diameter of ≈6 mm was used. This corresponds to a surface area of $\approx 4\times10^3$ Å^2 (about 400 sites) at a field emitter with ≈750 Å radius.

C. Titration reactions

1. The CO-precovered Pt surfaces at 300 K

The surface plane specificity of the reaction of $O_{2\,gas}$ with CO_{ad} is illustrated in FIM images of Fig. 3. The manifold of larger or smaller single crystal planes of the field evaporated end form of the Pt emitter is initially covered with CO_{ad} and not imaged by the O_2-imaging gas [Fig. 3(a),

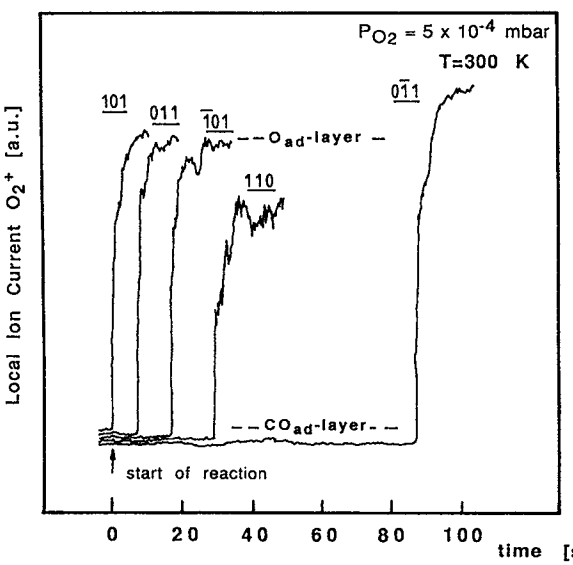

FIG. 4. The sequence of titration reactions for the different remote {011} planes, induction times, and titration rates in the reaction from CO_{ad} to O_{ad} layers.

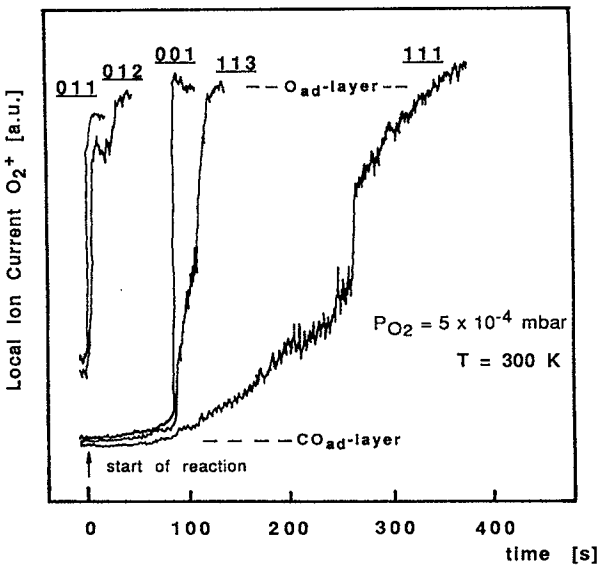

FIG. 5. The sequence of titration reactions for different single crystal planes in the reaction from CO_{ad} to O_{ad} layers at $T=300$ K.

where the orientation of low index planes is marked], after saturating the surfaces with $p_{CO}=10^{-5}$ mbar, for an extended time. Then oxygen with a partial pressure of $p_{O_2}=5\times10^{-4}$ mbar, is added at $\tau=0$ and the carbon monoxide is at the same time reduced to $p_{CO}\approx10^{-7}$ mbar. The sequence of video frames, presented in Fig. 3(a)–3(i), describes the surface selectivity of the reaction toward CO_2 and O_{ad}. The titration reaction starts at planes near {011} regions where the O_{ad} population is slowly growing up to a time where the (001) plane is quickly filled with O_{ad}. At prolonged times after filling diverse surface planes finally also the {111} planes are covered with O_{ad}.

The times required forming the O_{ad} coverage of the crystallographically identical but locally separated {011} planes are not synchronized. The delay times, presented in Fig. 4, show a counter-clockwise "switch-on" reaction sequence for the {011} planes starting with the (101) plane and followed by the (011), ($\bar{1}$01), (0$\bar{1}$1), and (110) plane. This shows nicely that all the {011} regions and in particular the surrounding {331} planes are activated first. Obviously, the pressure drop which is caused by the first "switch-on" reaction is insufficient to initiate gas phase synchronization at the other {011} surfaces.[8] The further population of {011} planes with oxygen in a counterclockwise sequence seems to be governed by mass transport at the surface, which must be a directed process, as to be discussed later on.

TABLE I. The reaction specificity of different planes of a Pt-field emitter at the titration reaction of a CO_{ad} layer with O_2 gas at $T=300$ K and $p_{O_2}=5\times10^{-4}$ mbar.

Planes Pt{hkl}	011	012	001	113	111
Induction time (s)	0	1	80	81	260
Rate of wave fronts (Å/s)	15	8	500	6	0.8

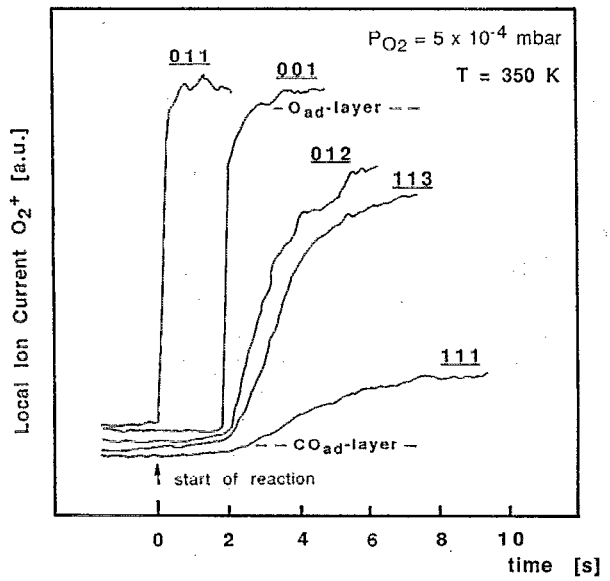

FIG. 6. The titration reaction of Fig. 5, now at $T=350$ K.

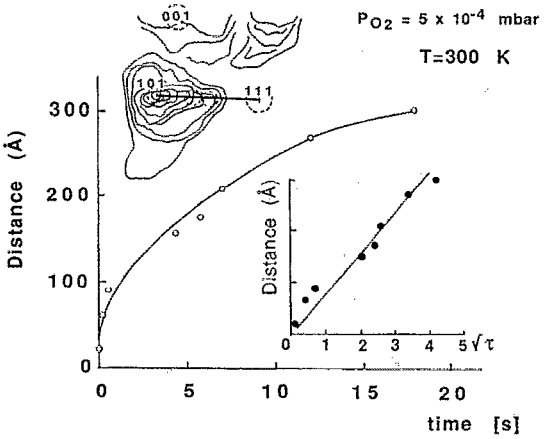

FIG. 7. The diffusion front of the titration reaction starting at the (101) plane; insert above: crystallographic orientation of the wave front, time dependence of the reaction front, linear $\sqrt{\tau}$ dependence in propagation rate (as insert on the right).

The reaction sequence for different single crystal orientations is displayed in Fig. 5. The initial start of the {011} and {012} planes is followed by a rather long delay (of ≈90 s) until a very quick titration reaction proceeds at the central (001) plane combined with a slower reaction on the {113} surfaces. The {111} planes display a different behavior. A very slow reaction is interrupted by an intermediate fast reaction followed by a further slow reaction which completes the O_{ad} layer on the {111} planes only after ≈400 s at 300 K. A summary of induction times and rates of wave fronts is given in Table I.

At elevated temperatures the titration reaction proceeds with much higher velocities. The delay times are reduced by more than an order of magnitude and the crystallographic specificity differs slightly (Fig. 6). For instance, the (012) plane now has a longer delay time than the (001) plane. Also

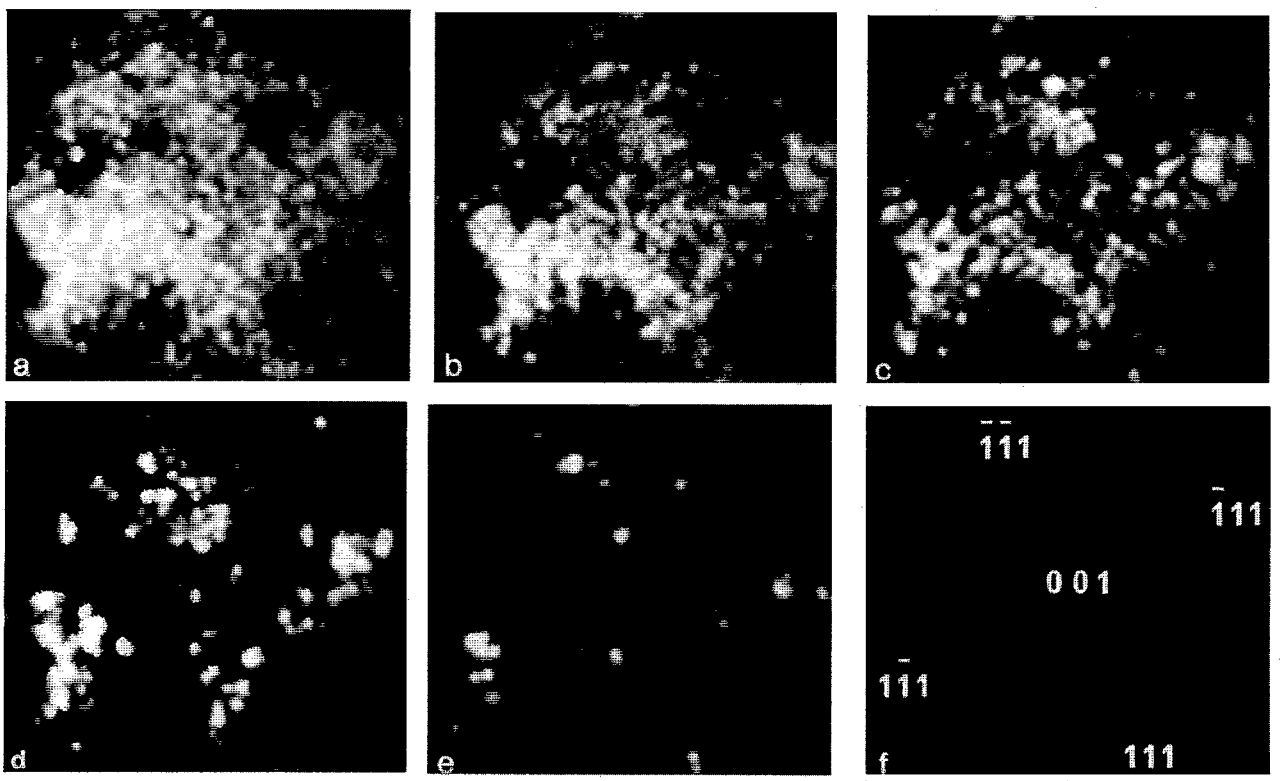

FIG. 8. FIM images of the titration reaction $O_{ad}+2\,CO_{gas} \rightarrow CO_{2\,gas}+CO_{ad}$. (a) O_2^+ image of O_{ad} sites, FIM at 15 kV, $F_{im} \cong 1.5$ V/Å, $p_{O_2} = 1 \times 10^{-5}$ mbar, $T=373$ K, $\tau=0$; (b) $\tau=21$ s after introduction of $p_{CO}=3\times10^{-5}$ mbar; (c) $\tau=25$ s; (d) $\tau=39$ s; (e) $\tau=70$ s; (f) $\tau=100$ s.

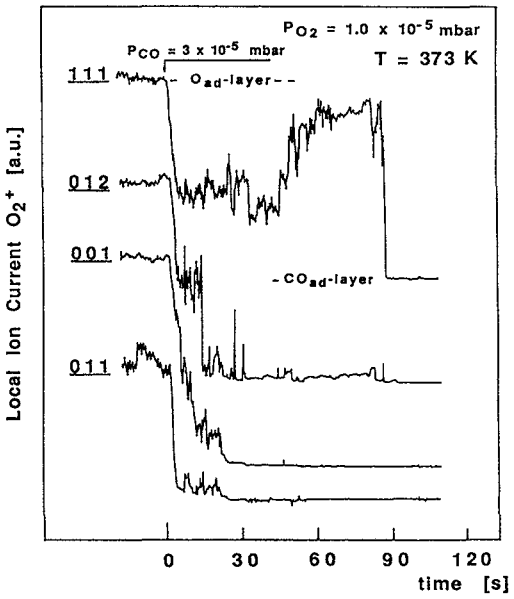

FIG. 9. The sequence of different crystal planes for the titration reactions $O_{ad} \rightarrow CO_{ad}$. Only minor differences are obtained for the small induction times of different single crystal planes. For the titration reaction at $T=373$ K, specific rates are observed for {012} and {111} planes.

the propagation rates of the wave fronts have higher values.

2. The anisotropy of wave fronts

The titration reaction of precovered CO_{ad} with oxygen adsorbing from the gas phase displays a pronounced anisotropy. At 300 K, starting from the (101) plane the wave front which shows the borderline between CO_{ad}—and O_{ad}—areas proceeds in the direction toward the (313) plane (Fig. 7). From there it turns into the (212) plane and finally into the (111) plane. During this motion of the wave front several surfaces—such as the (001) plane—are, as soon as they are touched by this front, quickly transferred into O_{ad} layers by a fast "switch-on" reaction. These switch-on reactions also display reaction diffusion wave fronts with rates given in Table I. The slower motion of the wave front on high index planes (Fig. 7) is governed by a diffusion process and follows a square root dependence as described in Fick's Law. The diffusion coefficient of the wave front, derived from the mean square displacement $\Delta r^2 = 4D\tau$, reaches a value of $D \approx 1.5 \times 10^3$ Å^2 s^{-1} which is nearly an order of magnitude smaller than the diffusion coefficient of CO on Pt at these conditions. Since oxygen atoms are rather immobile species on platinum surfaces at 300 K, we have to realize that CO_{ad} molecules diffuse in opposite direction of the wave front. The reaction at the wave front toward CO_2 gas forms empty sites which are occupied by dissociating O_2 molecules. The propagation of the wave front therefore is partially "eaten up" by the reaction. The observed velocity of the wave front is determined by a difference of rates, the diffusion rate of CO_{ad} toward the O_{ad}-layer diminished by the production rate of CO_2 at the phase boundary.

3. The precovered O_{ad} layer at 373 K

An experimental problem arises for the titration reaction of the precovered oxygen layer with gaseous CO. Since O_2 molecules are required as imaging gas the titration cannot be studied without allowing a certain partial pressure of oxygen ($p_{O_2} = 1 \times 10^{-5}$ mbar in the following). After introduction of $p_{CO} = 3 \times 10^{-5}$ mbar a certain competition between adsorption rates of carbon monoxide and of oxygen has to be taken into account. On the O_{ad}-precovered surface, the adsorption of CO is characterized by island formation which starts again in the {011} regions [Fig. 8(a)]. These islands grow quickly [Fig. 8(b)], wave fronts seem to propagate anisotropically. The field ion currents of different planes as evaluated from the local brightness of the video screen are displayed in Fig. 9. It is obvious that delay times are much less pronounced and less surface plane specific than before during the formation of O_{ad} layers. Within a few seconds the titration reaction of all surfaces is terminated, except for the {111} planes. Here, after a certain coverage with CO_{ad}, a back-reaction starts with a temporary increase of the field ion current until, after an extended time of $\tau > 90$ s, the CO_{ad} layer is formed in a very quick "switch-on"-reaction step. An interaction of the oxygen imaging gas during the titration reaction has to be considered at this plane.

III. DISCUSSION

Since the ingenious work of E. W. Müller[9] the imaging of individual atomic sites at solid surfaces by FIM has found many fruitful applications in material science, metallurgy, corrosion, and as well in surface chemistry.[10–12] The surface analysis of reactants, reaction intermediates, and products was performed in particular with field pulse- or photon pulse-field desorption mass spectrometry.[13] The *in situ* imaging of a surface reaction by using the reacting gas molecules directly as imaging gas has, however, so far not been experienced. The presumption of uncontrolled field effects probably was one of the reasons for this omission.

The present contribution proves that FIM can be an instrument that makes a chemical surface reaction directly visible on an atomic scale. On account of the particular conditions of field ion formation only those surface sites with adsorbed oxygen, O_{ad}, are imaged in the experiments. Thus, reaction centers which produce or consume O_{ad} during the CO oxidation can be located.

This *in situ* FIM of a surface reaction represents a new experimental tool with a so far unexplored potential for elucidating mechanisms of heterogeneous catalysis.

The experiments lead to some observations which are not understood satisfactorily. The field ionization process of oxygen as illustrated in Fig. 2 requires further theoretical considerations. The exclusivity in the imaging of O_{ad} sites on diversified Pt planes with widely varying work function values needs a profound explanation. It was an unexpected observation to see the O_{ad} sites under reaction conditions at low field strength values and in such a bright picture. May be local electric fields which have recently been discussed with local adsorption structures,[14] or interatomic interactions

("resonance states") contribute to this phenomenon of preferential field ionization of molecular oxygen at O_{ad} surface sites of platinum.

Furthermore, field effects have to be considered during the imaging of the surface by O_2^+ at a field strength of $\approx$1.5 V/Å. The Pt–O as well as the Pt–CO surface bond probably should already be altered by the external field, if experimental and theoretical data of other molecules, such as NO are compared.[15–18] Experimental results, however, show no significant field influences besides field compression of gas partial pressures. During the imaging process 10^2 to 10^3 O_2^+ ions/s are formed at each single O_{ad} surface site. One would expect that the same number of released tunneling electrons would interact with the O_{ad} layer and alter the adsorption structures. If for instance, the O_2^+ field ionization would proceed only few Å in front of the surface, electrons with few volts energy would hit and excite the adsorption layer and probably lead to the electron-stimulated field description process, ESFD.[19] None of these expected field effects was found. By unknown reasons, which require fundamental investigations, O_{ad} sites are obviously undisturbed while imaged by O_2^+-field ions.

Taking advantage of this phenomenon a pronounced surface specificity of the CO oxidation on platinum has been detected. Many detailed observations have to be understood in order to clarify the mechanism of the titration reactions.

Considering the precovered CO_{ad} surface during the titration with gaseous oxygen molecules, a preferential initiation of the reaction is always found in the {011} regions. The reason for this preference may be either given by thermochemical facts or by the dynamics of chemisorption processes. In the reaction $CO_{ad}+O_{2\,gas}\rightarrow CO_{2\,gas}+O_{ad}$ differences of the heat of adsorption of different planes O_{ad}, $\Delta H_{O_{ad}}$ could be important. Quantitative values of $\Delta H_{O_{ad}}$ for different Pt-crystal planes have so far not been evaluated systematically. On the other hand, sticking coefficients of oxygen and carbon monoxide at different single crystal planes are well known and may offer an explanation for the surface specificity.

The sticking coefficient (σ) of O_2 on the Pt(110)-1×2 plane is at 300 K between 0.3 and 0.6 for zero coverage Θ ($\sigma\approx$0.3 ... 0.6 for $\Theta=0$) and decreases until the saturation coverage $\Theta\approx$0.35 is reached.[20] Also the Pt(210) displays a high initial sticking coefficient ($\sigma\approx$0.5 at $\Theta=0$).[21] In comparison, the Pt(111) plane has a sticking coefficient which is one order of magnitude smaller (σ=0.06).[22] On the Pt(100) plane the initial sticking coefficient sensitively depends on the surface geometry. For the reconstructed Pt(100) hex a value of $\sigma=10^{-3}$ is found which changes to $\sigma\approx10^{-1}$ if the reconstruction is lifted for instance by CO_{ad}.[23] The surface specificity of the sticking coefficients may explain the sequence of titration reactions. In conclusion the {011} planes with the highest sticking probability for O_{ad} are expected to react first.

At the (001)-oriented field emitter tip [Fig. 3(b)] there are four {011} planes symmetrically located at distances of $\approx$500 Å around the central (001) plane and an additional (110) plane is visible with a greater distance of 1000 Å due to a grain boundary. The titration reaction of all these different CO-precovered surfaces is uncorrelated. Although the surface symmetry of these planes is identical and although the external control parameters are also the same, the reaction starts randomly only at one of the {011} planes; in Fig. 3 it is the (101) plane (at 7:00). It is unpredictable at which of these particular {011} planes the reaction will start first. For the then following {011} plane a simple rule is found. Always the nearest neighbored plane to the last reacting one is following. This rule, for instance, is found in a counterclockwise sequence in Fig. 3. Such a behavior seems to be due to the depletion of the CO_{ad} layer near the reaction border with CO consumption in the $CO_{2\,gas}$ formation. Empty surface sites are adsorbing O_{ad}. A slow diffusion of CO_{ad} toward the freshly formed rather immobile O_{ad} layer then determines the reaction sequence of the {011} planes in Fig. 4. After starting at the (101) plane the wave front of relatively immobile O_{ad} which receives supply from the gas phase moves toward the $(\bar{1}01)$, (110), and finally to the remote $(0\bar{1}1)$ plane in a counterclockwise circle. An important observation is that all the {011} planes—after the individual delay times—finally perform the reaction toward the O_{ad} layer in an extremely fast "switch-on" reaction. The removal of CO_{ad} by slow diffusion processes creates a situation where gaseous oxygen molecules suddenly gain a high sticking probability. For these results on (011) planes it is unlikely that faceting—as discussed for large single crystal planes[24]—is of importance. The reversible reaction behavior during many titration cycles excludes slow time-dependent faceting processes at 300 or 350 K.

Planes with different symmetry than (011) (Fig. 5) show much higher induction times. At T=300 K the (111) plane needs up to 400 s for completion of the titration reaction while the (011) planes [except $(0\bar{1}1)$ in Fig. 4] were covered in less than 30 s.

The titration reaction of CO_{ad} layers toward O_{ad} sites is governed by two competing processes: the oxygen adsorption from the gas phase near a CO_{ad} site and the surface diffusion of CO toward adsorbed oxygen, again with subsequent reaction to CO_2 at surface sites which then are empty and become available for further oxygen adsorption. With such a model one can qualitatively explain the results of Fig. 3. After initial adsorption of oxygen at the {011} planes diffusion of CO_{ad} from surrounding regions and reaction at the O_{ad}-island borderline lead to a depletion of CO_{ad} in surroundings [Fig. 3(a)–3(f)] until finally the subcritical CO coverage also at the (001) plane is reached and the "switch-on" reaction toward O_{ad} at the Pt(001) plane occurs by oxygen adsorption from the gas phase and by wave front propagation simultanously. A further diffusion process, as described in Fig. 7, finally leads to the reaction at the (111) planes, where the sticking coefficient (of the clean surface) is relatively small. A quantitative description of these processes is complicated by the fact that sticking and diffusion coefficients in each of the planes have a special dependence on CO_{ad} and O_{ad} coverages.

The titration reaction of O_{ad} with CO_{gas} on the other hand proceeds without noticeable induction times. This follows from the behavior of CO with high sticking coefficients at each of the Pt{hkl} planes. The CO molecule needs only

one adsorption site and therefore in some examples, for instance at the Pt(011) (CO) 2×1-structure the sticking coefficient of CO_{gas} is high even if oxygen is preadsorbed.[20] In Fig. 9, the transition from the O_{ad} layer to the CO_{ad} layer occurs simultaneously (within a few seconds) at all the investigated surface planes. The chemisorption of CO and consequently the titration reaction of O_{ad} with CO_{gas} seems to be a structure-insensitive process.

The present results of the titration reaction are in agreement with earlier results by FEM measurements. Also there it was found that the $CO+O_{ad}$ reaction proceeds at 360 K$<T<$420 K with highest rate in {110} planes with sharp boundary, which moves from {110} to {210} and {310} planes with activation energies of ≈4 kcal/mole.[25]

IV. SUMMARY

TABLE II. The results of the titration reactions.

	$CO_{ad}+O_{2\,gas}$ reaction	$O_{ad}+CO_{gas}$ reaction
Reaction temperature	300–380 K	300–373 K
Surface plane specifity	Most active {110} Least active {111}	Reaction with CO_{gas} begins in region of {110} plane
Induction time	Small at {110} {210} Middle at {100} High at {111}	Absent
Existence of a reaction boundary	Boundary start at (110) and moves to (113)→(210)→(111)	Chaotic growth of CO_{ad}-island boundaries without crystallographic specifity
Rate of wave fronts	Very fast at (100)-plane	Comparably much smaller
Mechanism of wave propagation	Surface mobility of CO_{ad} molecules	Growth of CO_{ad} islands at proceeding titration reaction with mobile CO_{ad}
Mechanism of sharp boundary appearance	Adsorption and dissociation of impinging O_2 molecules at immobile O_{ad}-island boarders	Disappearance at the immobile layer

ACKNOWLEDGMENTS

We thank M. Ehsasi for valuable discussions. V.G. acknowledges a fellowship of the Max-Planck-Gesellschaft.

[1] G. Ertl, Adv. Catal. **37**, 213 (1990).
[2] F. Schüth, B. E. Henry, and L. D. Schmidt, Adv. Catal. **39**, 51 (1992).
[3] R. Imbihl (in press); Prog. Surf. Sci. **44**, 185 (1994).
[4] V. Gorodetskii, J. H. Block, W. Drachsel, and M. Ehsasi, Appl. Surf. Sci. **67**, 198 (1993).
[5] J. H. Block, M. Ehsasi, and V. Gorodetskii, Prog. Surf. Sci. **42**, 143 (1993).
[6] V. Gorodetskii, W. Drachsel, and J. H. Block, Catal. Lett. **19**, 223 (1993).
[7] M. Bär, Ch. Zülicke, M. Eiswirth, and G. Ertl, J. Chem. Phys. **96**, 8595 (1992).
[8] M. Ehsasi and J. H. Block, *Proceedings of the International Conference on Unsteady State Processes in Catalysis*, Novosibirsk/Russia, edited by Yu. Sh. Matros (VSP Netherlands, 1990), p. 47.
[9] E. W. Müller, Z. Phys. **131**, 136 (1951).
[10] T. Sakurai, A. Sakai, and H. W. Pickering, Adv. Electron. Electron Phys. Suppl. **20** (1989).
[11] M. K. Miller and G. D. W. Smith, *Atom Probe Microanalysis* (Material Research Society, Salem, MA, 1989).
[12] T. T. Tsong, *Atom Probe Field Ion Microscopy* (Cambridge University, Cambridge, 1990).
[13] J. H. Block, G.-K. Chuah-Jaenicke, and N. Kruse, *Surface Science of Catalysis—In Situ Probes and Reaction Kinetics*, edited by D. J. Dwyer and F. H. Hoffmann (ACS Symp. Series 482, Washington, DC 1992), p. 287.
[14] Yu Suchorski, W. A. Schmidt, and J. H. Block, Proc. 39th Int. Field Emission Symp., Halifax/Canada 1992, Appl. Surf. Sci. **67**, 124 (1993).
[15] H. J. Kreuzer, in *Chemistry and Physics of Solid Surfaces*, edited by R. Vanselow (Springer Berlin, 1990), p. 133.
[16] J. H. Block, H. J. Kreuzer, and L. C. Wang, Proc. 37th Int. Field Emission Symp., Albuquerque, NM, 1990; Surf. Sci. **246**, 125 (1991).
[17] R. P. Madenach, G. Abend, M. S. Mousa, H. J. Kreuzer, and J. H. Block, Proc. 38th Int. Field Emission Symp., Wien, Austria, 1991; Surf. Sci. **266**, 56 (1992).
[18] R. P. Madenach, G. Abend, H. J. Kreuzer, and J. H. Block, Ber. Bunsenges. Phys. Chem. (to be published).
[19] N. Ernst and J. H. Block, Surf. Sci. **117**, 561 (1982).
[20] M. Eiswirth, Dissertation, LMU Munich, 1987.
[21] M. Ehsasi, Dissertation, FU Berlin, 1989.
[22] P. R. Norton, K. Griffith, and P. E. Binder, Surf. Sci. **138**, 125 (1984).
[23] R. J. Behm, P. A. Thiel, P. R. Norton, and G. Ertl, J. Chem. Phys. **78**, 7437 (1983).
[24] M. Sander and R. Imbihl, Surf. Sci. **255**, 61 (1991).
[25] V. Gorodetskii and V. I. Savchenko, Dokl. Akad. Nauk SSSR **15**, 336 (1974); UDC **541**, 183 [in English].